Acta Epileptologica

RESEARCH Open Access

SiRNA-mediated ankyrin-G silence modulates the expression of voltage-gated Na channels in murine hippocampal HT22 cells

Guanzhong Ni[1†], Xiaoting Hao[2†], Xiaodong Cai[1,3], Jiaming Qin[1], Liemin Zhou[1,4], Patrick Kwan[1,5] and Ziyi Chen[1*]

Abstract

Background: Voltage-gated sodium channels are the targets of many commonly used antiepileptic drugs. $Na_V1.6$, encoded by *Scn8a*, increased in chronic mesial temporal epilepsy animal models and co-localized with Ankyrin-G, encoded by *Ank3*. We hypothesized that inhibition of *Ank3* transcription by siRNA decrease the expression of $Na_V1.6$.

Results: We characterized expression of the target genes in hippocampal neuron HT22 cells by Real time-PCR. The melt peak in the resolution curve of *Scn1a*, *Scn8a* and *Ank3* were all unique. *Ank3* transcription was interfered and the relative *Ank3* mRNA levels of the three interfered groups compared to GAPDH were 0.89 ± 0.13, 0.52 ± 0.07 and 0.26 ± 0.05 while that of the negative control group was 1.01 ± 0.08 ($P < 0.05$). When *Ank3* transcription was inhibited by siRNA, the relative mRNA levels of *Scn8a* decreased in the three groups (0.91 ± 0.09, 0.33 ± 0.06 and 0.25 ± 0.05), compared to the negative control group (1.10 ± 0.09). Tested by Western blotting, protein levels of ankyrin-G and Nav1.6 decreased after *ank3*-siRNA. Ankyrin-G in negative control group, group1, group2 and group1 + 2 were 0.813 ± 0.051, 0.744 ± 0.041, 0.477 ± 0.055 and 0.351 ± 0.190 respectively ($P < 0.01$) while Nav1.6 were 0.934 ± 0.036, 0.867 ± 0.078, 0.498 ± 0.070 and 0.586 ± 0.180 ($P < 0.01$). The quantity analysis of immunofluorescence showed significant decrease of ankyrin-G and Nav1.6 (Student's test, $P = 0.046$ and 0.016 respectively).

Conclusion: We therefore concluded that in HT22 cells the expression of Nav1.6 was down-regulated by *Ank3* RNA interference.

Keywords: Nav1.1, Nav1.6, Ankyrin-G, Hippocampal neurons, HT22

Background

Drug resistance in epilepsy is the failure of adequate trials of two appropriately chosen, well tolerated and used antiepileptic drug schedules to achieve seizure freedom [1]. The biological mechanisms underpinning pharmacoresistance in epilepsy remain unclear. One of the proposed mechanisms, coined the "target hypothesis", postulates that resistance to antiepileptic drugs results from alteration of their molecular targets [2].

Voltage-gated sodium channels (VGSC) are known to play a central role in excitability and signaling in neurons, and targets of many commonly used antiepileptic drugs. The VGSC family contains ten α-subunits, such as $Na_V1.1$ encoded by *SCN1A* and $Na_V1.2$ encoded by *SCN2A*, with different sodium currents biophysical properties and locations. *SCN1A*, *SCN2A* and *SCN8A* were all frequently mutated gene in drug-resistant pediatric epilepsies [3]. The antiepileptic drugs are not specific to the isoforms of voltage-gated sodium channels [4]. Therefore, selective targeting of a specific voltage-gated isoform may provide an improvement in drug resistance.

We previously reported that $Na_V1.6$ expression is increased in hippocampal cornu ammonis 1 subfield in chronic mesial temporal epilepsy animal models while

* Correspondence: chenziyi22@hotmail.com
Guanzhong Ni and Xiaoting Hao are the co-first-author.
[1]Department of Neurology, National Key Clinical Department and Key Discipline of Neurology, the First Affiliated Hospital, Sun Yat-sen University, Guangzhou, China
Full list of author information is available at the end of the article

$Na_V1.1$ remained stably expressed, suggesting that $Na_V1.6$ might be the major α-subunit involved in the chronic epilepsy mechanism [5]. Several studies demonstrated the relationship between Nav1.6 and persistent sodium currents: in CA1 pyramid cells from mice with a truncated nonfunctional form of NaV1.6, persistent sodium currents were significantly reduced [6]; in a mice model with complete loss of NaV1.6 expression, the persistent sodium currents were significantly reduced, compared to the wild type [7]; tsA201 cells transfected with the human Nav1.6 cDNA exhibited significant persistent sodium current [8]. Further study of amydgala-kindled rats reported that increase of *Sca8n* expression was observed in the CA3 region of the hippocampus, which was associated the persistent sodium currents and the enhancement of the neuronal repetitive firing capacity [9]. Mutation of the mouse *Scn8a* gene which reduce the expression of Nav1.6 can resistant to amygdala kindling [4]. These results raised the possibility that selective modulation of Nav1.6 expression may provide a new angle to solve drug resistance in epilepsy treatment.

VGSC location in plasma membrane depends on the protein-protein interaction and intracellular trafficking. Ankyrin-G, a neuronal skeletal protein encoded by *ANK3*, has been investigated for transferring neuronal membrane ion channels such as sodium channels and potassium channels [10, 11]. Ankyrin-G links voltage-gated sodium channels and adhesion molecules with C-terminal regulatory domains to the actin cytoskeleton via spectrins [12]. Ankyrin-G regulates neuronal excitability by reducing the persistent sodium currents of $Nav1.6^8$ and over-expression of the complex Shank3 including ankyrin-G was demonstrated of spontaneous seizure and partial lethality in mice [13]. We have previously reported that ankyrin-G and $Na_V1.6$ co-localized and both increased significantly in the cornu ammonis 1 subfield of the rat hippocampus 60 days following pilocarpine induced status epilepticus, which indicated a suppression by ankyrin-G to Nav1.6 was present during the chronic spontaneous stage [5]. However, it is unknown whether the increase of $Na_V1.6$ and ankyrin-G is a coincidental phenomenon or is causally related.

We hypothesized that inhibition of *Ank3* transcription by siRNA decrease the expression of $Na_V1.6$. In this study we studied the endogenous expression of ankyrin-G and voltage-gated sodium channels in the hippocampal HT22 cell line and effects of siRNA knockdown of ankyrin-G on the expression of sodium channels.

Results

Positive expression of *Scn1a*, *Scn8a* and *Ank3* in HT22 cell line down-regulation of Scn8a by the knockdown of *Ank3*

First of all, we characterized expression of the target genes in hippocampal neuron HT22 cells by Real time-PCR. The melt peak in the resolution curve of *Scn1a*, *Scn8a Ank3* and *GAPDH* were all unique and the melting points of the genes were respectively 82 °C, 78.3 °C, 83.5 °C and 82.6 °C (Additional file 1: Figure S1), which suggested the immortalized HT22 cells could be used in the further study of relationship of ankyrin-G and the two sub-types of voltage-gated sodium channels.

The efficacy of siRNA transfection was investigated. We constructed two different *Ank3* siRNA sequences targeting *Ank3* mRNA. The relative *Ank3* mRNA levels of the three interfered groups compared to GAPDH were 0.89 ± 0.13, 0.52 ± 0.07 and 0.26 ± 0.05 while that ofnegative control (NC) group was 1.01 ± 0.08 (Fig. 1). The transfection rate was 11.89, 48.51 and 74.26%, compared to NC group. The analysis revealed a significant change in gene expression after siRNA interference (One-way ANOVA $F = 9.520$, $P < 0.05$). However, the inter-groups Student's test revealed no significant difference between NC group and group1 ($t = 1.417$, $P = 0.229$) while significant difference was detected between NC group and group2 ($t = 4.406$, $P = 0.01$) and between NC group and group1 + 2 ($t = 4.345$, $P < 0.01$). The two-step comparisons of gene silencing efficiency demonstrated that the second sequence of *Ank3* siRNA interfere the expression of *Ank3* successfully.

We next tested whether *Ank3* knockdown result in the alteration of sodium channel subunits. The relative mRNA level of *Scn1a* of HT22 cells after the interference of siRNA of *Ank3* remained relative stable. Similar decreasing trend was found in *Scn8a* expression after siRNA interference compared to that of *Ank3*. The relative mRNA levels of *Scn8a* in group1, group2 and group1 + 2 were respectively 0.91 ± 0.09, 0.33 ± 0.06 and 0.25 ± 0.05 while that of NC group was 1.10 ± 0.09 (Fig. 1). The analysis revealed a significant change in *Scn8a* gene expression after siRNA interference (One-way ANOVA $F = 10.577$, $P < 0.01$). The Bonferroni's

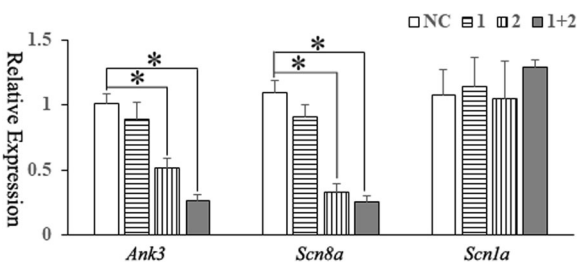

Fig. 1 mRNA levels of *Ank3*, *Scn8a* and *Scn1a* after siRNA interference. The relative *Ank3* mRNA levels decreased significantly after siRNA interference in group 2 and group 1 + 2. The expression of *Scn8a* decreased $69.9 \pm 8.4\%$ in group2 ($P < 0.05$) and $77.3 \pm 4.1\%$ in group1 + 2($P < 0.05$). The relative mRNA level of *Scn1a* of HT22 cells after the interference of siRNA of *Ank3* remained relative stable

tests of Post-hoc analysis confirmed the significant difference between group 2/group1 + 2 and NC group but no statistic difference between group1 and NC control. The expression of *Scn8a* decreased 18.8 ± 9.3% in group 1($P = 0.055$), 69.9 ± 8.4% in group2 ($P < 0.05$) and 77.3 ± 4.1% in group1 + 2($P < 0.05$).There was no statistical significant between NC group and the other three groups (1.08 ± 0.19, 1.14 ± 0.23, 1.05 + 0.29 and 1.29 ± 0.06, one-way ANOVA F = 0.797, $P = 0.529$) (Fig. 1).

Protein levels of ankyrin-G, Nav1.6 and Nav1.1 after the knockdown of *Ank3*

Western blotting approach was performed to examine the alterations of ankyrin-G, Nav1.6 and Nav1.1 protein level after siRNA interference (Fig. 2). Nav1.6 and Nav1.1 protein was identified as an immunopositive band with molecular weight around 260 kDa. Ankyrin-G was identified around 190 kDa. GAPDH was around 146 kDa. We measured the Integral optical density value (IDV) and found that the relative IDV of ankyrin-G protein compared to that of GAPDH in NC group, group1, group2 and group1 + 2 were 0.813 ± 0.051, 0.744 ± 0.041, 0.477 ± 0.055 and 0.351 ± 0.190 respectively (one-way ANOVA F = 4.676, $P < 0.01$). Compared to NC group, the IDV of ankyrin-G protein was revealed 41.3 ± 2.7% decrease in group2($P < 0.05$) and 56.8 ± 2.9% decrease in group1 + 2($P < 0.05$) but only 9.28 ± 1.9% decrease in group 1 ($P = 0.051$). These data indicated again that the second sequence of *Ank3*-siRNA silenced the expression of ankyrin-G successfully.

The quantitative analysis detected significant alteration in Nav1.6 protein level after *Ank3*-siRNA interference. Relative IDV of Nav1.6 protein compared to that of GAPDH in NC group, group1, group2 and group1 + 2 were 0.934 ± 0.036, 0.867 ± 0.078, 0.498 ± 0.070 and 0.586 ± 0.180 respectively (one-way ANOVA F = 5.826, $P < 0.01$). The relative IDV of Nav1.6 of HT22 cells decreased 46.7 ± 3.1% in group2 ($P < 0.05$) and 37.3 ± 1.9% decrease in group1 + 2 ($P < 0.05$). Relative IDV of Nav1.1 protein compared to that of GAPDH in NC group, group1, group2 and group1 + 2 were 0.776 ± 0.111, 0.801 ± 0.048, 0.785 ± 0.086 and 0.775 ± 0.072 respectively (one-way ANOVA F = 0.605, $P = 0.63$). No significant difference was found in Bonferroni's test of Post-hoc analysis.

Immunoreactivity of ankyrin-G, Nav1.6 and Nav1.1 after the knockdown of *Ank3*

To determine whether the alteration of ankyrin-G mRNA transcript expression and protein level correlated to the changes of its immunoreactivity and the localization of Nav1.6 and Nav1.1 in HT22 neurons, we developed immunofluorescence attaining assays for direct detection. The pattern of Nav1.6 and Nav1.1 immunoreactivity was described in hippocampal pyramidal cells [14]. We observed similar patterns of Nav1.6, Nav1.1 and ankyrin-G immunofluorescence staining in NC group and interference group as membrane proteins. After the interference both ankyrin-G and Nav1.6 decreased and no positive illuminant detection were found in axon initial segment (Fig. 3). The quantity analysis of normalized integrated density detected significant decrease of the immunofluorescence of Ankyrin-G and Nav1.6 (Student's test, $P = 0.046$ for ankyrin-G; $P = 0.016$ for Nav1.6) after siRNA interference compared to NC group. No difference of the immunofluorescence of Nav1.1 existed compared to NC group (Student's test, $P = 0.085$).

Discussion

In this study we reported that the positive expression of *Scn1a*, *Scn8a* and *Ank3* in HT22 cell line and down-regulation of the membrane sodium channel subunit Nav1.6 by silencing *Ank3* expression using siRNA while the expression of Nav1.1 was not affected.

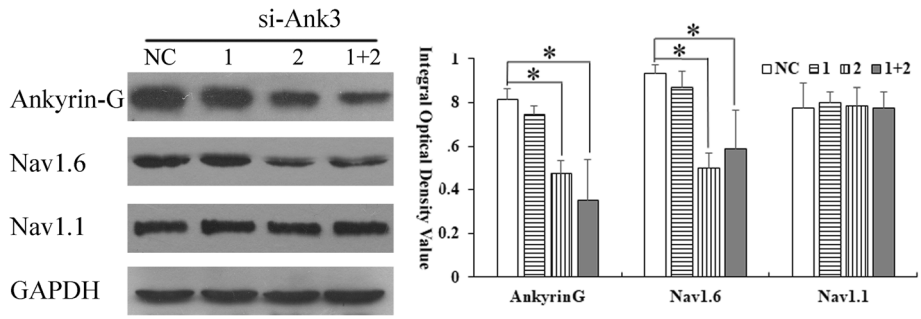

Fig. 2 Protein levels of Ankyrin-G, Nav1.6 and Nav1.1 after siRNA interference in HT22 cells. Ankyrin-G, Nav1.6, Nav1.1 and GAPDH were detected as the immunopositive bands with molecular weight around 190 kDa, 260 kDa, 260 kDa and 146 kDa respectively. We found similar changes of ankyrin-G and Nav1.6 IDV protein level after siRNA silence in group2 and group1 + 2

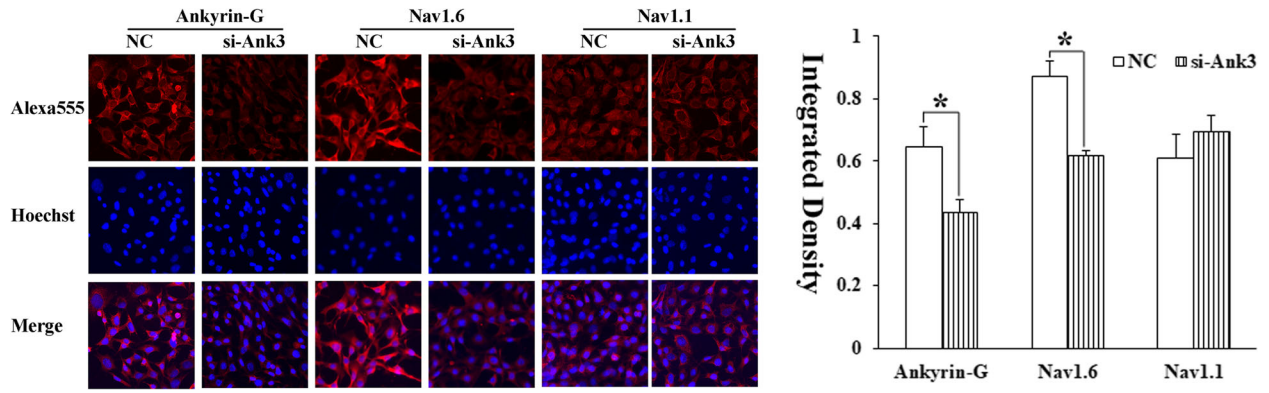

Fig. 3 Immunocellularchemistry assay for Ankyrin-G, Nav1.6 and Nav1.1 after siRNA interference in HT22 cells. In the representative sections, antibodies illustrate the localizing of Ankyrin-G, Nav1.6 and Nav1.1 labeled with Alexa555 in red and nuclei were revealed by Hoechst in blue. Quantification of Ankyrin-G revealed significant decrease of normalized integrated density after siRNA silence compared to NC group ($P < 0.05$). Similar change of integrated density of Nav1.6 were detected ($P < 0.05$)

Positive expression of *Scn1a*, *Scn8a* and *Ank3* in HT22 cell line

In vitro cellular models have been playing an important role in the studies about cellular and molecular mechanisms in epilepsy and its drug resistance. Nowadays several types of cells have been used in the studies of the mechanism of membrane channels, such as human embryonic kidney 293T [15], TsA201 cells [8], neuroblastoma and neuron hybrid [10] and Xenopus oocytes [16]. Hippocampus sits in the center because mesial temporal lobe epilepsy is one of the most common syndromes of both children and adults. Furthermore, hippocampal sclerosis is strongly associated with drug resistant epilepsy. Therefore, it is necessary to seek a cell model originated from hippocampal neurons, besides those without hippocampal features like human embryonic kidney 293 T and tsA201 cells.

Among the established neuronal cell lines, the HT22 is a widely used hippocampal neuronal cell line in a variety of studies such as apoptosis, dementia, and brain tumor [17–19]. The cell line is superior for the biophysical characteristics of hippocampal neurons; therefore, it might be preferred in the research for epilepsy and antiepileptic drugs. HT22 were sublined cloned from HT4 cells, which were immortalized from the primary murine hippocampal neurons [20]. In this study, the melting curves of *Ank3*, *Scn1a*, *Scn8a* and GAPDH in HT22 cells demonstrated the expression of mRNAs encoding *Ank3*, *Scn1a*, *Scn8a* and GAPDH in HT22 cells (Additional file 1: Figure S1). We demonstrated the expression of *Ank3*/ankyrin-G, *Scn1a*/Nav1.1 and *Scn8a*/Nav1.6 at detectable levels using real-time PCR and Western blotting. These results suggested that the cell line might be used as a cell model for the study of these sodium channels and their modulators.

The culture of primary hippocampal neurons is a mature method [10, 11]. Compared with the acute isolation neurons, cell lines are abundant, stable, efficient for molecular-biological and neurophysiological researches.

siRNA interfering to *scn8a* expression

In the present study the reduction of *Ank3* expression by siRNA was accompanied by reduced mRNA level of *Scn8a* and protein level of Nav1.6, while the expression of *Scn1a* was unchanged. These results provide strong evidence that down regulation of ankyrin-G affects the expression of Nav1.6 without affecting that of Nav1.1.

We have previously shown increasing expression of *Scn8a* in hippocampal cornu ammonis 1 during the spontaneous seizure stage of chronic epileptic animal models, which mediated persistent sodium currents in the region and involved in epileptogenesis [5]. In this study we performed the siRNA experiment to demonstrate that ankyrin-G directly down-regulated the expression of *Scn8a*. The modulation of ankyrin-G was reported in studies in other cells and tissues. For example, ankyrin-G was required for maturation and maintenance of Ranvier's Nodes [21]. Alteration in the ankyrin-G pathway for targeting Nav1.5 to the intercalated disc was associated with Brugada syndrome [22, 23]. In this study we focused on the hippocampal neurons and explored the alteration of sodium channel isoforms after suppression of *Ank3*. We can see similar effects of ankyrin-G to voltage gated sodium channels in different types of neurons and myocardial cells. With the previous reports, it supported to the hypothesis that expression level and function of *Scn8a* may be regulated by ankyrin-G with different orientation.

The previous expression studies showed robust persistent sodium currents with hNav1.6 cDNA transfected in Xenopus oocytes [16], human embryonic kidney cells [15] and tsA201 cells [8]. Ankyrin-G significantly reduced persistent sodium currents of hNav1.6 channels [8]. Increasing persistent sodium currents may exacerbate repetitive discharge of hippocampal neurons and decrease neuronal electrical stability which might be involved in the mechanism of epileptogenesis and the development of drug-resistance [4]. Ankyrin-G co-localized with *Scn8a* also increased, which might inhibit persistent sodium currents of *Scn8a* and restrain the development of epilepsy. Therefore, inhibition of ankyrin-G may down-regulate the expression of *Scn8a* in hippocampus and the alteration of the latter may induce the decline of persistent sodium currents in quantity.

We found no effect of *Ank3*-siRNA on the expression of *Scn1a*. Recent studies have provided compelling evidence for a complex cell specific sub-domain organization of VGSCs subunits with a spatially and temporally defined expression pattern [24]. Different subunits of VGSCs are expressed in different regions of the central nervous system and peripheral nervous system. VGSC subunits expression may change during neuro-development, such as the neonatal phase, mature phase, and physiopathologic phase of epilepsy [24]. In this study we observed that ankyrin-G played different roles in modulation of expression between the subunit Nav1.6 and Nav1.1 of VGSC.

There were some limitations in our studies. First of all, we compared the regulation of ankyrin-G on the two isoforms of VGSC subunits. Future studies should evaluate the effect of ankyrin-G on other VGSC subunits and other membrane channel proteins in the reorganized network during the development of epilepsy and drug resistance. The role of other proteins composing the macro-molecular complexes that may be involved in the interaction of ankyrin and VGSC, such as βIV spectin, CK2, neurofascin [11, 25, 26], should also be investigated in the epileptogenesis and the development of new antiepileptic drugs. Second, in terms of developing ankyrin-G as a potential target of intervention, the effects of ankyrin-G on the intracellular traffic, localization and functional modulation of other ion channels and membrane protein should be considered and investigated. Thirdly, further electrophysiological studies are needed to confirm the regulation to functions of the sodium channels.

Conclusions

HT22 cells with detectable expression levels of *Ank3*/ankyrin-G, *Scn1a*/Nav1.1 and *Scn8a*/Nav1.6 may be used as a cell model for the study of these sodium channels and their modulators. The expression of Nav1.6 was down-regulated by *Ank3* interference in this cell model.

Methods

Cell culture

HT22 cells, derived from parent HT4 cells that were originally immortalized from primary mouse hippocampal neuronal culture, were kindly provided by Prof. J. Liu [16]. The HT22 cell strains were cultured in Dulbecco's modified Eagle's medium (DMEM) supplied with 10% fetal bovine serum at 37 °C in a humidified atmospheric chamber with 5% CO_2.

SiRNA-mediated interference

We used vector-based small-interfering RNA (siRNA) strategy to suppress the endogenous ankyrin-G expression in the cultured murine hippocampal neurons. The siRNA constructs were obtained from GenePharma (Shanghai, China). Two siRNA sequences were selected to knockdown ankyrin-G expression in HT22 neurons according to the sequences predicted to produce significant alignments at the website of National Center of Biotechnology Information (NM_03180). The sequences targeting *Ank3* by the siRNA were 5'TTCCCAAAGTAC AGGAGGT 3′ and 5'GGCAGACAGACGCCAGAGC3', which were demonstrated to be specific in a previous study [27]. To exclude potential off-target effect we double-checked the sequences' specificity with BLAST and dscheck [28, 29].

The cells were randomly separated into 4 groups: Negative control group (NC group), group1 (interfered with the first siRNA sequence), group 2 (interfered with the second siRNA sequence) and group 1 + 2 (interfered with both sequences simultaneously). Cells were seeded at a density of 50% on six-well plates with serum-free culture medium 24 h prior to transfection. Prepared 100 nM siRNA complexes was mixed with 250 μl Opti-MEM (Invitrogen, USA) by gently shaking and 10 μl lipofectamin™ 2000(Invitrogen, USA) was dissolved in 250ul Opti-MEM. After standing for 5 min, the solutions of siRNA and lipofectamin™ 2000 was added to the cells. Then the cells were incubated at 37 °C and 5% CO2. The medium was changed 4 h after transfection and cells were incubated for another 48 h in the 5% fetal bovine serum till they were washed with phosphate buffer saline buffer and harvested for analysis of *Ank3*, *Scn1a* and *Scn8a* expression by real-time Polymerase Chain Reaction (rt-PCR), immunohistochemistry (IH) staining and Western Blotting (WB).

Quantitative real-time PCR analysis

Cultured HT22 Cells treated with siRNA in the plate were lysed and homogenized for total RNA extraction

with Trizol (TR118–500, Molecular Research Center, Inc. Cincinnati, OH, USA). First strand cDNA was synthesized from 2 μg of total RNA with M-MLV Reverse Transcriptase (M1705, Promega Madison, WI, USA). Rt-PCR cycles were carried out for amplification of *Ank3*, *Scn1a* and *Scn8a* through the MiniOpticon Real-Time PCR Detection System (Bio-Rad Laboratories, Inc., Hercules, CA, USA). Primers of target genes and the house-keeping gene glyceraldehyde-3-phosphate dehydrogenase (GAPDH) were designed and synthesized by Shanghai Generay Biotech Co (Table 1). The cDNA (1.5 μl) was amplified in a 20 μl reaction volume containing 10 μl of GoTaq® qPCR Master Mix (Promega Madison, WI, USA), 6.5 μl Nuclease-Free Water and 1 μl of the respective forward and reverse primers. An eppendorf containing all the components except the template DNA was used as a negative control. PCR was initiated with a Hot-start activation step at 95 °C for 2 min followed by 40 cycles at 95 °C for 3 s and annealing/Extension at 60 °C for 30 s, at last incubated for dissociation program at 60–95 °C. We set up the program with a melting curve analysis performed after the final cycle to demonstrate the unique product was amplified. We applied Pfaffl's comparative method of quantitative real-time-PCR program to compare gene expressions of the target genes with that of the "house-keeping" gene with the following formula.

$$\text{Ratio} = \left((E_{\text{Target}})^{\Delta Ct_{(\text{Target})}^{(\text{control}-\text{sample})}}\right) / \left((E_{\text{ref}})^{\Delta Ct_{(\text{ref})}^{(\text{control}-\text{sample})}}\right)$$

E_{Target} was the amplification efficiency of target gene RNA in real-time fluotescence PCR while E_{ref} was that of reference gene RNA.$\Delta Ct_{(\text{Target})}$ was the difference of Ct of control (NC group) and sample (siRNA group) for target gene while$\Delta Ct_{(\text{Ref})}$ meant Ct of control minus that of sample for hose-keeping gene.

Western blotting analysis

The primary antibodies used in immunocytochemistry and Western blotting were anti-Nav1.1 and anti-Nav1.6 from Millipore (Temecula, CA, USA), and anti-Ankyrin-G Mouse mAb and GAPDH from Invitrogen (Camarillo, CA, USA).Total proteins were extracted from cells of each group with RIPA/Laemmli Buffer (Bio-Rad Laboratories Inc. Hercules, CA) and ultrasonic. Protein concentrations are determined with the Micro BCA™ protein Assay Reagent (Pierce Biotechnology, Rockford, IL, USA). After SDS-PAGE gel electrophoresis on a 6% stock gel and 10% separate gel, proteins were transferred to polyvinylidene fluoride membrane. After being blocked in 5% fresh non-fat milk (Amresco, Solon, OH, USA) with shaking, the membrane was incubated with primary antibody anti-Nav1.1 (1:200), anti-Nav1.6 (1:200), anti-ankyrin-G (1:800) and anti-GAPDH (1:1000) overnight at 4 °C followed by anti-Rabbit secondary antibody (KPL Inc., Gaithersburg, MD, USA). Proteins were detected by luminol chemiluminescent substrate (Cell Signalling, Danvers, MA, USA) and band intensities were quantified by ImageJ 1.48v software (Bethesda, MD, USA).

Immunocellularchemistry

We chose the cells of group2 comparing with negative control group for immunofluorescent experiments. Cells were blocked with 3% normal goat serum at room temperature for 1 h and incubated with primary antibodies, including anti-Nav1.1 (1:200) and anti-Nav1.6 (1:200) and Anti-Ankyrin-G (1:1000) overnight at 4 °C and with the Alexa Fluor® 555 Donkey Anti-Rabbit secondary antibodies (Invitrogen, Camarillo, CA, USA) at room temperature for 1 h. After phosphate buffered saline rinsing, cells were incubation with Hoechst33258 (1:1000, from Invitrogen, Camarillo, CA, USA)) for 10 min. Negative controls were incubated with 0.01 M phosphate buffered saline in place of the primary antibody. Fluorescence signals were detected with a microscope (Axio Imager Z1, ZEISS) at excitation/ emission wavelengths of 555/565 nm (Alexa Fluor 555, red) and 346/460 nm (Hoechst 33258, blue). Quantification was performed using ImageJ 1.48v software (Bethesda, MD, USA). Image stacks were converted into 8 bit and inverted before the integrated density was measured.

Statistical analysis

All data were analyzed with SPSS16.0 (SPSS Inc., Chicago, IL, USA). The numerical values were presented as mean ± SD. Student's t tests were used to compare between groups. One-way ANOVA was carried out for multiple groups comparisons followed by Bonferroni's post-hoc analysis. $P < 0.05$ was considered statistically significant.

Table 1 Sequences of Forward and reverse primers for real-time PCR

Target genes	Forward sequences(5′-3′)	Reverse sequences(5′-3′)
MZ-*Ank3*	GGCCTTACCCCAATCCATGTT	TCCTTAGCTTTTGCTTCTACCTG
MZ-*Scn8a*	GCAAGCTCAAGAAACCACCC	CCGTAGATGAAAGGCAAACTCT
MZ-*Scn1a*	TCAGAGGGAAGCACAGTAGAC	TTCCACGCTGATTTGACAGCA
MZ-GAPDH	AGGTCGGTGTGAACGGATTTG	TGTAGACCATGTAGTTGAGGTCA

Additional file

Additional file 1: Figure S1. The melting curves of *Ank3*, *Scn1a*, *Scn8a* and *GAPDH* in HT22 cells. The melt peak in the resolution curve of *Scn1a*, *Scn8a Ank3* and *GAPDH* were all unique and the melting points of the genes were respectively 82 °C, 78.3 °C, 83.5°Cand 82.6 °C. The curves suggested the immortalized HT22 cells could be used in the further study of relationship of ankyrin-G and the two sub-types of voltage-gated sodium channels. (TIF 4095 kb)

Abbreviations

GAPDH: Glyceraldehyde-3-phosphate dehydrogenase; IDV: Integral optical density value; siRNA: small-interfering RNA; VGSC: Voltage-gated sodium channel

Acknowledgements

We thank Prof. Jun Liu in the second affiliated Hospital of san Yat-sen University for the general award of HT22 cell line. We appreciate Dr. Howan Leung's writing assistance and prof. Yi Zhou's statistical help.

Authors' contributions

GN, XH, LZ and ZC contributed experiment design. GN performed the siRNA interference. XC performed Western blotting. XH performed the PCR and JQ did immunocytochemistry experiments. ZC drafted the article and PK revised the manuscript critically. All authors read and approved the final manuscript.

Authors' information

No other information is supplemented.

Funding

The study was supported by the National Nature Science foundation (81000554), Guangdong Nature Science foundation (2018A030313345) and the Science and Technology Foundation of Guangdong Province (2008B030301058).

Availability of data and materials

The data and material were unconcealed.

Ethics approval and consent to participate

This was a study based on cell line. No human or animals were involved. Therefore, there was neither ethics approval nor consent to participate.

Consent for publication

No conflict of interest exits in the submission of this manuscript, and the manuscript is approved by all authors for publication.

Competing interests

The authors declare that they have no competing interests.

Author details

[1]Department of Neurology, National Key Clinical Department and Key Discipline of Neurology, the First Affiliated Hospital, Sun Yat-sen University, Guangzhou, China. [2]Department of Neurology, West China Hospital, Sichuan University, Chengdu, China. [3]Department of Neurology, the Sixth Affiliated Hospital, Sun Yat-sen University, Guangzhou, China. [4]Department of Neurology, the Seventh Affiliated Hospital, Sun Yat-sen University, Guangzhou, China. [5]Department of Neurology, Royal Melbourne Hospital, University of Melbourne, Melbourne, Australia.

Received: 25 January 2019 Accepted: 6 August 2019
Published online: 31 August 2019

References

1. Kwan P, Arzimanoglou A, Berg AT, et al. Definition of drug resistant epilepsy: consensus proposal by the ad hoc task force of the ILAE commission on therapeutic strategies. Epilepsia. 2010;51:1069–77.
2. Kwan P, Schachter SC, Brodie MJ. Drug-resistant epilepsy. N Engl J Med. 2011;365:919–26.
3. Parrini E, Marini C, Mei D, et al. Diagnostic targeted resequencing in 349 patients with drug-resistant pediatric epilepsies identifies causative mutations in 30 different genes. Hum Mutat. 2017;38:216–25.
4. Makinson CD, Tanaka BS, Lamar T, Goldin AL, Escayg A. Role of the hippocampus in Nav1.6 (Scn8a) mediated seizure resistance. Neurobiol Dis. 2014;68:16–25.
5. Chen Z, Chen S, Chen L, et al. Long-term increasing co-localization of SCN8A and ankyrin-G in rat hippocampal cornu ammonis 1 after pilocarpine induced status epilepticus. Brain Res. 2009;1270:112–20.
6. Royeck M, Horstmann MT, Remy S, Reitze M, Yaari Y, Beck H. Role of axonal NaV1.6 sodium channels in action potential initiation of CA1 pyramidal neurons. J Neurophysiol. 2008;100:2361–80.
7. Enomoto A, Han JM, Hsiao CF, Chandler SH. Sodium currents in mesencephalic trigeminal neurons from Nav1.6 null mice. J Neurophysiol. 2007;98:710–9.
8. Shirahata E, Iwasaki H, Takagi M, et al. Ankyrin-G regulates inactivation gating of the neuronal sodium channel, Nav1.6. J Neurophysiol. 2006;96:1347–57.
9. Blumenfeld H, Lampert A, Klein JP, et al. Role of hippocampal sodium channel Nav1.6 in kindling epileptogenesis. Epilepsia. 2009;50:44–55.
10. Akin EJ, Sole L, Dib-Hajj SD, Waxman SG, Tamkun MM. Preferential targeting of Nav1.6 voltage-gated Na+ channels to the axon initial segment during development. PLoS One. 2015;10:e0124397.
11. Hedstrom KL, Ogawa Y, Rasband MN. AnkyrinG is required for maintenance of the axon initial segment and neuronal polarity. J Cell Biol. 2008;183:635–40.
12. Nelson AD, Caballero-Floran RN, Rodriguez Diaz JC, et al. Ankyrin-G regulates forebrain connectivity and network synchronization via interaction with GABARAP. Mol Psychiatry. 2018. https://doi.org/10.1038/s41380-018-0308-x.
13. Jin C, Zhang Y, Kim S, Kim Y, Lee Y, Han K. Spontaneous seizure and partial lethality of juvenile Shank3-overexpressing mice in C57BL/6 J background. Mol Brain. 2018;11:57.
14. Catterall WA, Goldin AL, Waxman SG. International Union of Pharmacology. XLVII. Nomenclature and structure-function relationships of voltage-gated sodium channels. Pharmacol Rev. 2005;57:397–409.
15. Burbidge SA, Dale TJ, Powell AJ, et al. Molecular cloning, distribution and functional analysis of the NA(V)1.6. Voltage-gated sodium channel from human brain. Mol Brain Res 2002;103:80-90.
16. Smith MR, Smith RD, Plummer NW, Meisler MH, Goldin AL. Functional analysis of the mouse Scn8a sodium channel. J Neurosci. 1998;18:6093–102.
17. Liu J, Li L, Suo WZ. HT22 hippocampal neuronal cell line possesses functional cholinergic properties. Life Sci. 2009;84:267–71.
18. Park SY, Jin ML, Kim YH, Kim CM, Lee SJ, Park G. Involvement of heme oxygenase-1 in neuroprotection by sanguinarine against glutamate -triggered apoptosis in HT22 neuronal cells. Environ Toxicol Pharmacol. 2014;38:701–10.
19. Kempf SJ, Buratovic S, von Toerne C, et al. Ionising radiation immediately impairs synaptic plasticity-associated cytoskeletal Signalling pathways in HT22 cells and in mouse brain: an in vitro/in vivo comparison study. PLoS One. 2014;9:e110464.
20. Morimoto BH, Koshland DE Jr. Induction and expression of long- and short-term neurosecretory potentiation in a neural cell line. Neuron. 1990;5:875–80.
21. Saifetiarova J, Taylor AM, Bhat MA. Early and late loss of the cytoskeletal scaffolding protein, Ankyrin G reveals its role in maturation and maintenance of nodes of Ranvier in myelinated axons. J Neurosci. 2017;37:2524–38.
22. El Refaey MM, Mohler PJ. Ankyrins and Spectrins in cardiovascular biology and disease. Front Physiol. 2017;8:852.
23. Makara MA, Curran J, Little SC, et al. Ankyrin-G coordinates intercalated disc signaling platform to regulate cardiac excitability in vivo. Circ Res. 2014;115:929–38.
24. Leterrier C, Brachet A, Dargent B, Vacher H. Determinants of voltage-gated sodium channel clustering in neurons. Semin Cell Dev Biol. 2011;22:171–7.
25. Hien YE, Montersino A, Castets F, et al. CK2 accumulation at the axon initial segment depends on sodium channel Nav1. FEBS Lett. 2014;588:3403–8.
26. Hedstrom KL, Xu X, Ogawa Y, et al. Neurofascin assembles a specialized extracellular matrix at the axon initial segment. J Cell Biol. 2007;178:875–86.

27. Ayalon G, Davis JQ, Scotland PB, Bennett V. An ankyrin-based mechanism for functional organization of dystrophin and dystroglycan. Cell. 2008;135:1189–200.
28. Yamada T, Morishita S. Accelerated off-target search algorithm for siRNA. Bioinformatics. 2005;21:1316–24.
29. Naito Y, Yamada T, Matsumiya T, Ui-Tei K, Saigo K, Morishita S. dsCheck: highly sensitive off-target search software for double-stranded RNA -mediated RNA interference. Nucleic Acids Res. 2005;33:W589–91.